University of South Carolina College of Engineering and Computing Mechanical Engineering Department

Nano- and Microstructures for Thin-Film Evaporation—A Review

J. L. Plawsky, A. G. Fedorov, S. V. Garimella, H. B. Ma,S. C. Maroo, L. Chen, and Y. Nam

Nanoscale and Microscale Thermophysical Engineering, 18: 251–269, 2014

ISSN: 1556-7265 print / 1556-7273 online
DOI: 10.1080/15567265.2013.878419

NANO- AND MICROSTRUCTURES FOR THIN-FILM EVAPORATION—A REVIEW

J. L. Plawsky[1], A. G. Fedorov[2], S. V. Garimella[3], H. B. Ma[4], S. C. Maroo[5], L. Chen[6], and Y. Nam[7]

[1]*Department of Chemical & Biological Engineering, Rensselaer Polytechnic Institute, Troy, New York*
[2]*The George W. Woodruff School of Mechanical Engineering, Georgia Institute of Technology, Atlanta, Georgia*
[3]*School of Mechanical Engineering, Purdue University, West Lafayette, Indiana*
[4]*Department of Mechanical and Aerospace Engineering, University of Missouri, Columbia, Missouri*
[5]*Department of Mechanical and Aerospace Engineering, Syracuse University, Syracuse, New York*
[6]*Department of Mechanical Engineering, University of South Carolina, Columbia, South Carolina*
[7]*Department of Mechanical Engineering, Kyung Hee University, Yongin, Gyeonggi, Korea*

Evaporation from thin films is a key feature of many processes, including energy conversion, microelectronics cooling, boiling, perspiration, and self-assembly operations. The phase change occurring in these systems is governed by transport processes at the contact line where liquid, vapor, and solid meet. Evidence suggests that altering the surface chemistry and surface topography on the micro- and the nanoscales can be used to dramatically enhance vaporization. The 2013 International Workshop on Micro- and Nanostructures for Phase-Change Heat Transfer brought together a group of experts to review the current state-of-the-art and discuss future research needs. This article is focused on the thin-film evaporation panel discussion and outlines some of the key principles and conclusions reached by that panel and the workshop attendees.

KEY WORDS: wetting, evaporation, nanostructure, microstructure, heat transfer

INTRODUCTION

Nearly 50 years ago, Derjagin et al. [1] performed an experiment and demonstrated that the rate of evaporation from walls of a capillary tube was enhanced by isothermal liquid flow in the thin film of liquid that clung to the walls of a capillary. The driving force behind this excess liquid flow was attributed to a gradient in the long-range intermolecular

Manuscript received 9 September 2013; accepted 5 December 2013.
Address correspondence to J. L. Plawsky, Department of Chemical & Biological Engineering, Rensselaer Polytechnic Institute, Troy, NY 12180. E-mail: plawsky@rpi.edu
Color versions of one or more of the figures in the article can be found online at www.tandfonline.com/umte.

force field. Calculations on this kind of moving meniscus for example, in conical capillaries, were given by Kiseleva et al. [2]. Shrage, in his monograph [3], developed a theoretical framework for modeling interphase transport that has served as a guide for researchers for over 60 years. This early work led to extensive research on the flow in thin films that are one to two orders of magnitude larger than the adsorbed films usually associated with surface diffusion. Controlling the transport processes in these films using surface modification techniques has become a very important area of research in the fields of enhanced heat and mass transfer, coating technology, and self-assembly processes.

Great strides have been made in understanding the nature of solid–liquid–vapor interactions atop a nano- or microstructured solid surface. Much of this understanding has arisen from the discovery of naturally occurring biological surfaces that use chemical and topographical features to control the interaction of fluids with their surfaces (see Figure 1). Researchers have successfully developed many forms of superhydrophobic [4–6], superhydrophilic [7–9], and omniphobic [5, 10] surfaces designed to mimic biological surfaces and operate isothermally. Others have fabricated omniphobic surfaces to probe interesting features for phase-change heat and mass transfer [11]. Despite these efforts, the full potential of such surfaces for heat and mass transfer applications has just begun to be explored.

Surface patterns formed either by chemical modification or by additive or sacrificial structural features alter three interrelated phenomena that can affect phase change [12]. The size and morphology of the surface features created define which solid/liquid/vapor

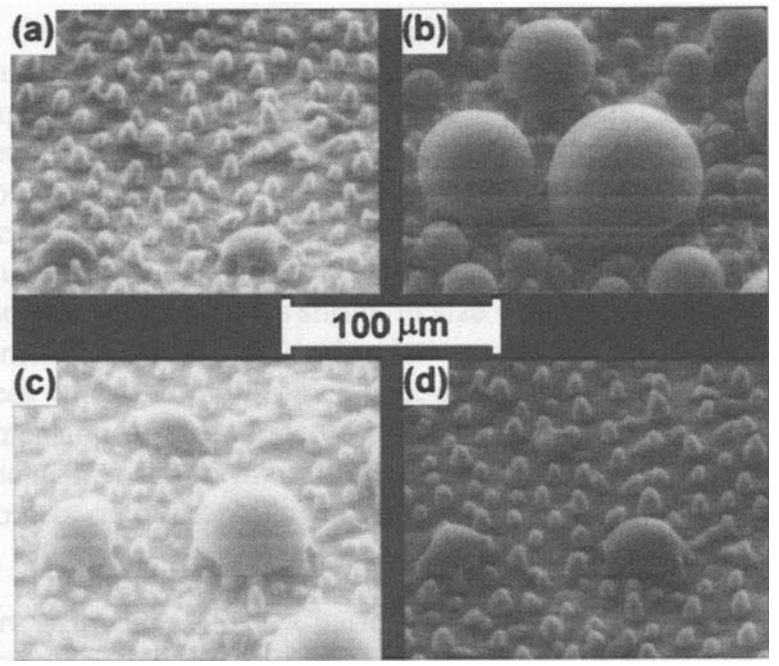

Figure 1 (a), (b) Condensation and (c), (d) evaporation from a lotus leaf [88]. Reprinted with permission from Y.-T. Cheng, D.E. Rodak, A. Angelopoulos, and T. Gacek, Microscopic Observations of Condensation of Water on Lotus Leaves, *Applied Physics Letters*, Vol. 87, pp. 194112−194113, 2005. Copyright 2005, AIP Publishing LLC.

interactions are enhanced or diminished. Techniques that change the interfaces on a macroscopic scale have been used for a very long time to increase the contact area between the heat transfer fluid and the underlying solid [13]. Micrometer-sized features lead to a similar increase in solid–liquid interfacial area, but they also act as capillary wicking agents [14–16] and may increase the number of nucleation sites for enhancing change of phase heat transfer [17–19]. The surface energy of the solid may be altered by chemical modification or by using submicrometer- or nanosized structures [12, 21–26]. When this surface energy change occurs, the wetting behavior of the liquid changes and, as a result, fluid flow processes on the surface are altered. Finally, submicrometer- and nanosized structures can also serve to increase the adsorbed film thickness and to increase hydrodynamic slip at the solid–liquid interface [27–29]. Experimental results and observations from biological systems both point to the advantage of a hierarchical surface structure to achieve maximum performance in phase-change processes [12].

Changes in surface chemistry and the addition of surfactants or other secondary liquid species can also exert strong effects on phase change processes [25, 30]. The addition of fluid dopants allows one to alter the Marangoni stresses at the liquid–vapor interface and hence alter the flow of liquid from the bulk to the contact line region [31–35]. All modification processes, whether physical or chemical, have the same purpose—maximizing the region where phase change is most active. Though great strides have been made, much work remains to be done to develop surfaces that can be tailored for any particular liquid–solid combination.

THIN-FILM EVAPORATION FUNDAMENTALS

To understand how surface modification affects thin-film evaporation processes, we need to understand the fundamentals of phase-change transport in thin films. Though work in this area began with Derjagin and colleagues [1], many others have contributed from the experimental [36–43], theoretical [44–48], and simulation [49–56] perspectives. Evaporation from thin films is nearly always in the context of an evaporating meniscus. For simplicity, if we consider the case of a perfectly wetting fluid, one can divide an evaporating meniscus into three hypothetical regions (see Figure 2). Region 1 is the *adsorbed/nonevaporating film region* that is a precursor to the apparent contact line where liquid, vapor, and solid are assumed to meet. This adsorbed/nonevaporating film is of uniform thickness and cannot evaporate due to the combined effects of attractive forces between the solid and the liquid, vapor pressure, and substrate temperature. Region 2 is the *transition region* where the attractive forces of the solid are much weaker and the liquid–vapor interface has measurable curvature. During active evaporation, the gradient in the thickness and the curvature of the liquid–vapor interface drives the flow of liquid towards this region via capillary and intermolecular forces. Region 3 is the *bulk fluid* or *meniscus region* where the curvature of the interface becomes nearly constant. This region acts as a reservoir that feeds liquid to the transition region. The slope of the vapor–liquid interface at the start of this region defines what is usually reported as the contact angle.

The heat transfer process can be analyzed in terms of these three regions and their associated thermal resistances. In the simplest case of a static meniscus, there are three resistances in series: (1) a conduction resistance through the solid substrate, generally small due to the high conductivity of the solid material; (2) a conduction resistance through the liquid that is a linear function of the film thickness; and (3) a liquid–vapor interfacial heat transfer resistance. The interfacial resistance depends on the strength of the intermolecular

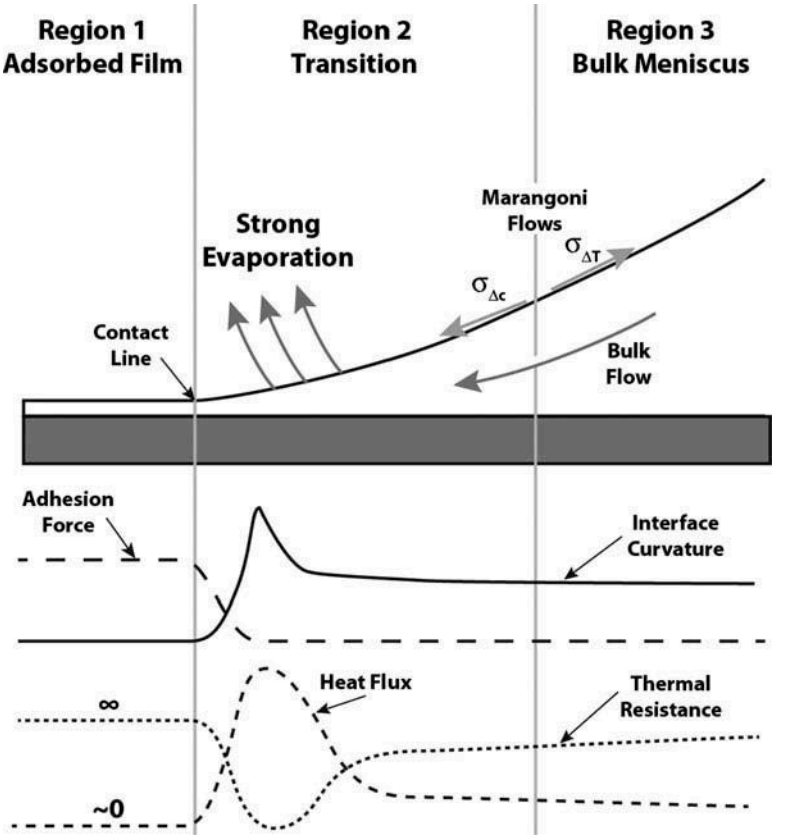

Figure 2 Variation in adhesion force, curvature, heat flux, and thermal resistance in the contact line region for an evaporating meniscus.

forces and hence the film thickness, the curvature of the vapor–liquid interface, and the state of the bulk vapor. This resistance can be the dominant thermal resistance in the system especially for liquids having a very high latent heat of vaporization or systems where the surface area between liquid and solid is extremely high.

A qualitative depiction of the thermal resistance network along the evaporating meniscus is shown in Figure 2. The overall thermal resistance in the adsorbed film is effectively infinite because there is no evaporation in this region. The resistance in the bulk fluid region can also be very high due to a large conduction resistance through the relatively thick liquid film. The thermal resistance reaches a minimum in the transition region. In this region, the comparatively thin liquid film thickness imposes a moderate conduction resistance, yet the film thickness is large enough so that the interfacial resistance decreases rapidly as the film thickens. These features have been observed experimentally [36–43] and simulated numerically by a number of researchers [44–56].

The heat transfer resistances are only part of the entire story. There are hydrodynamic resistances that provide fundamental limits to how fast a molecule of vapor can be added into an already occupied vapor space (sonic limit) [57], to how thin a liquid film can be before that film either becomes temporally unstable or ruptures [58–60], and to how much liquid can be delivered to the active evaporation zone either through flow in a thin

film (a wetting/friction limit), through an intrinsic meniscus (capillary limit) or through a structure such as a wick [8, 15, 61–71] (a capillary/friction limit). The key to maximizing phase-change heat transfer would seem to be maximizing the region where the overall heat transfer resistance is lowered while at the same time minimizing the hydrodynamic resistances associated with pumping liquid into that region and pumping vapor out from that region.

The conceptual analysis presented above also applies to partially wetting liquids and fluid mixtures. Those systems can be quite a bit more complicated, especially if polar or ionic interactions are present. In general, partially wetting liquids have much thinner adsorbed films and those films are much less stable than the perfectly wetting case. Thus, the mix between heat transfer resistances would be different, the hydrodynamic resistances would be different, the film thickness profiles would be different, and perhaps even the phase behavior of the mixtures would be altered. However, the general concepts shown in Figure 2 would remain the same.

If we were dealing with nonwetting liquids, such as mercury, in confined geometries, the fundamental geometry represented by this thin-film evaporation analysis would no longer hold. In fact, there would be no meniscus and the problem would likely become dominated by conduction to the entire liquid–vapor interface (and the relative need to evaluate the interface resistance is lessened, depending on the length scale).

Evaporation from a meniscus is a very complicated, multiscale process. A convenient way to understand the variables governing phase change phenomena in this situation is to consider the problem from a thermodynamics perspective. The variation in chemical potential per unit volume, $\Delta\mu_g$, is composed of several components [72]:

$$\Delta\mu_{g,i}\left(\frac{J}{m^3}\right) = \rho_{lm}R_gT_{lv}\ln\left(\frac{P_{vlv}}{P_v}\right) = \underbrace{-(\Pi)}_{\text{Intermolecular}} - \underbrace{\sigma_{lv}K}_{\text{Surface}} + \underbrace{\frac{\rho_l\Delta h_{fg}}{\overline{T}}(T_{lv}-T_v)}_{\text{Thermal}} + \sum_i \underbrace{\frac{\rho_l R_g T}{M_w}\ln\left(\frac{x_i}{x_{i,ref}}\right)}_{\text{Concentration}} + \underbrace{\rho_l g z}_{\substack{\textit{Gravitational}\\ \textit{potential}}} - \underbrace{z_i c_i F E}_{\substack{\textit{Electrical}\\ \textit{potential}}}, \tag{1}$$

where P_v is the bulk vapor pressure; P_{vlv} is the vapor pressure at the vapor–liquid interface at some height, z, above the reservoir; ρ_{lm} is the liquid molar density (mol/m^3); ρ_l is the liquid density (kg/m^3); z_i is the valence of liquid species, i, if it can dissociate into ions; x_i is the concentration of the ith species; and $x_{i,\text{ref}}$ is the reference concentration of that species in the bulk fluid. The interfacial free energy is affected by the surface curvature (capillary pressure, $\sigma_{lv}K$), the adhesion forces (disjoining pressure, Π), the hydrostatic head ($\rho_l g z$), the temperature jump across the interface ($\Delta T = T_{lv} - T_v$), the concentration difference across the interface $\ln\left(x_{j,i}/x_{j,i,ref}\right)$, and any other externally applied fields, such as the electric field, E [73]. The product of the density ρ_l and the latent heat of vaporization, Δh_{fg}, is the volumetric heat of vaporization at the average phase change temperature, $\overline{T}$. If multiple fluids are present, we have an expression similar to Eq. (1) for each species.

The intermolecular component, represented by the disjoining pressure, Π, is composed of at least two parts, the Van der Waals component and a second component that handles all other forces. Following Basu and Sharma [74] we can express the disjoining pressure in the DLVO approximation as

$$\Pi = 64 c_{i\infty} k_b T \tanh\left(\frac{e\zeta_1}{4k_bT}\right)\tanh\left(\frac{e\zeta_2}{4k_bT}\right)\exp(-\kappa\delta) + \frac{A\left(15.96\left(\frac{\delta}{\lambda}\right)+2\right)}{12\pi\delta^3\left[1+5.32\left(\frac{\delta}{\lambda}\right)\right]^2}, \quad (2)$$

where T is the temperature, k_b is Boltzmann's constant, e is the fundamental charge, κ is the Debye length, λ is the London wavelength, ζ is the zeta potential with subscripts 1 and 2 signifying the two interacting surfaces, $c_{i\infty}$ is the ion concentration in the bulk liquid, and A is the Hamaker constant. Dzyaloshinskii, Lifshitz, and Pitaevskii's theory as discussed by Israelachvili [75] relates the Hamaker constant to the dielectric properties of the media involved. In the simplest approximation, we can relate the Hamaker constant to the refractive indices of the media involved (η_i) and the primary electronic absorption frequency that generally lies in the ultraviolet ($\nu_e \sim 3 \times 10^{15}$ s^{-1}, $\lambda \sim 100$ nm). This representation is given in Eq. (3) where the numerical subscripts represent the three media interacting (solid, liquid, vapor), ν is the electronic frequency of interaction, k_b is Boltzmann's constant, $\hbar$, is Planck's constant, and T is the temperature.

$$A = A_{\nu=0} + A_{\nu>0} = \frac{3}{4}k_bT\left(\frac{\varepsilon_1-\varepsilon_3}{\varepsilon_1+\varepsilon_3}\right)\left(\frac{\varepsilon_2-\varepsilon_3}{\varepsilon_2+\varepsilon_3}\right) + \frac{3\hbar\nu_e}{8\sqrt{2}}\left\{\frac{\left(\eta_1^2-\eta_3^2\right)\left(\eta_2^2-\eta_3^2\right)}{\left(\eta_1^2+\eta_3^2\right)^{1/2}\left(\eta_2^2+\eta_3^2\right)^{1/2}\left[\left(\eta_1^2+\eta_3^2\right)^{1/2}+\left(\eta_2^2+\eta_3^2\right)^{1/2}\right]}\right\}. \quad (3)$$

We can relate the intermolecular component to the interfacial tension and the contact angle using Eq. (4). Here, P_c is the pressure associated with the adsorbed film of thickness, δ_0. This equation is useful if we need to predict the contact angle for partially wetting liquids and for perfectly wetting fluids where, based on the film thickness profile, we can predict the apparent contact angle that arises under intense evaporation.

$$\cos\theta = 1 + \frac{1}{\sigma_{lv}}\int_0^{P_c}\delta d\Pi. \quad (4)$$

Supplying heat to a meniscus drives the system from equilibrium where kinetic theory may be used to obtain the rate of evaporation. The maximum rate of evaporation can be expressed in terms of the thermodynamic driving forces across the interface as determined from Eq. (2) [57]. Considering only thermal, intermolecular, capillary, and gravitational driving forces, we find the heat flux q'' to be a function of temperature and pressure jumps across the interface.

$$q'' = m''\Delta h_{fg} = h_{lv}\left(T_{lv}-T_v\right) = \frac{\left(T_{lv}-T_v\right)}{1/h_{lv}^{cl}} - \frac{\left(\Pi+\sigma_l K-\rho_l g z\right)}{1/h_{lv}^{kl}}, \quad (5)$$

where

$$h_{lv}^{kl} = \left(\frac{C^2M_w}{2\pi R_g T_{lv}}\right)^{(1/2)}\frac{V_{lm}P_v\Delta h_{fg}}{R_gT_{lv}} \quad (6)$$

and

$$h_{lv}^{cl} = \left(\frac{C^2 M_w}{2\pi R_g T_{lv}} \right)^{(1/2)} \frac{M_w P_v \Delta h_{fg}^2}{R_g T_{lv} T_v}. \tag{7}$$

Here, C is a proportionality constant of O(1), M_w is the molecular weight of the fluid, R_g is the universal gas constant, and Δh_{fg} is the heat of vaporization of the fluid. The classical heat transfer coefficient, h_{lv} in Eq. (5), presumes the evaporation rate is due to a temperature jump only. It is replaced here by the coefficients due to the temperature (h_{lv}^{cl}) and pressure (h_{lv}^{kl}) jumps, both of which contribute to evaporation. The pressure jump can be obtained from geometric considerations (measurements of thickness and curvature). The temperature jump at this scale is extremely difficult to determine. Usually one replaces it with the temperature difference between the solid surface and the bulk vapor augmented by a penalty function that may be just the conduction resistance through the liquid. The value of C, often referred to as the accommodation coefficient, is not a complete unknown in this analysis. Many careful experiments have been performed to measure this coefficient for a number of working fluids under controlled conditions, and the variation in measured values is primarily observed for water [76]. Of course, the coefficient itself becomes uncertain if there are noncondensible components in the gas phase or we have a liquid mixture where we need to consider relative volatilities of the components and the possibility that interfacial compositions are not equivalent to compositions in the bulk of the liquid film.

Though the electrostatic contribution to the forces has been typically ignored, a recent study by Narayanan et al. [61] of evaporation in a confined nanopore environment critically assessed this approximation and analyzed the combined effects of electrostatic interactions and Van der Waals forces. This study demonstrated a significant change in the shape of the interface due to electrostatic forces that extended the contact line especially within the nanoscale-sized pores. As a result, the net rate of evaporation was promoted due to an increase in the total free surface area, as well as due to an enlarged thin-film region in the meniscus.

The contact line or interline region (between the adsorbed film and evaporating film in Figure 2) is the thinnest portion of the meniscus over which evaporation can occur and hence it is also the location where the heat flux is the highest. In this nanoscale region, continuum models begin to break down and so molecular dynamics is required to understand the evaporation process (Figure 3) [52]. We can roughly use the Knudsen number as a gauge to when the continuum theory will fail. The molecular simulations show that an ultrahigh heat flux, on the same order as the kinetic theory limit, can occur in the interline region of a nanoscale meniscus (Figure 3). Because the interline region covers an extremely small area compared to the evaporating region, its impact on the overall heat transfer is not significant. However, increasing its area through novel nanostructured surfaces can significantly increase the heat flux at the device level. Moreover, this analysis can further be extended and applied to create ultrahigh heat flux energy conversion devices where evaporation (without nucleate boiling) is the only mode of phase change.

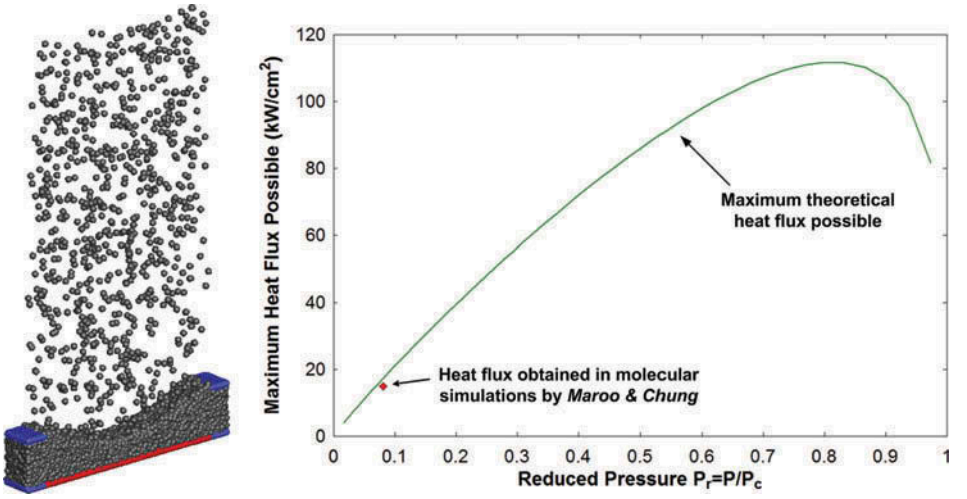

Figure 3 Comparison of molecular dynamics versus kinetic theory predictions for the maximum rate of evaporation from a thin film [52]. Reprinted from *International Journal of Heat and Mass Transfer*, Vol. 53, S.C. Maroo and J.N. Chung, Heat Transfer Characteristics and Pressure Variation in a Nanoscale Evaporating Meniscus, pp. 3335–3345, Copyright (2010), with permission from Elsevier.

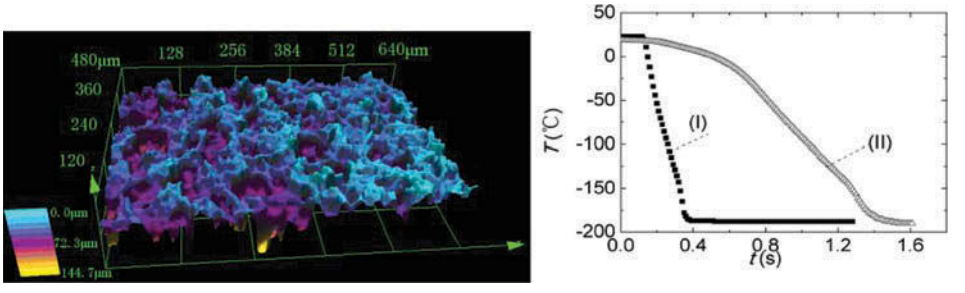

(a) (b)

Figure 4 Microstructured surface to increase the contact line region for enhanced heat transfer: (a) photo of microstructures by 3D laser scanning confocal microscopy and (b) histories of test section by (I) thin-film evaporation and (II) pool boiling (the test section was directly plunged in liquid nitrogen).

MICRO- AND NANOSTRUCTURES FOR CONTROLLING EVAPORATION

A wide range of surface modification strategies have been tried in an attempt overcome the obstacles [68, 69] preventing us from achieving the theoretical maximum evaporation rate. One such method using surface treatment to generate microstructured roughness is shown in Figure 4 [40].

Confining a microscopic liquid film using capillary forces exerted via nanoporous alumina membranes, as shown in Figure 5, to maximize and control (i.e., avoid surface dry-out) the rate of evaporation has been successfully pursued as an approach for cooling small areas subjected to high heat fluxes [61, 77–79]. Several investigations have numerically characterized evaporation from idealized microstructure geometries [65, 68] and realistic sintered microstructures via microtomography-based direct simulation (Figure 6) [61, 62]. Techniques for characterization of phase change from sintered porous media, as well as

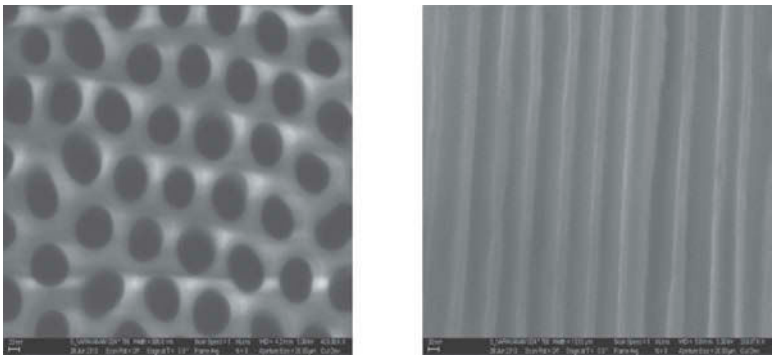

(a) (b)

Figure 5 Combining micro- and nanostructures via confining a thin liquid film of microscopic dimensions using a porous alumina membrane (PAM), whose cylindrical nanopores control phase-change operations. Scanning electron micrographs of the PAM: (a) top view and (b) cross-sectional cut along the pore axis [80]. Reprinted from *International Journal of Heat and Mass Transfer*, S. Narayanan, A. Fedorov, and Y. Joshi, Heat and Mass Transfer during Evaporation of Thin Liquid Films Confined by Porous Membrane Subjected to Air Jet Impingement, Vol. 58, pp. 300−311, Copyright (2013), with permission from Elsevier.

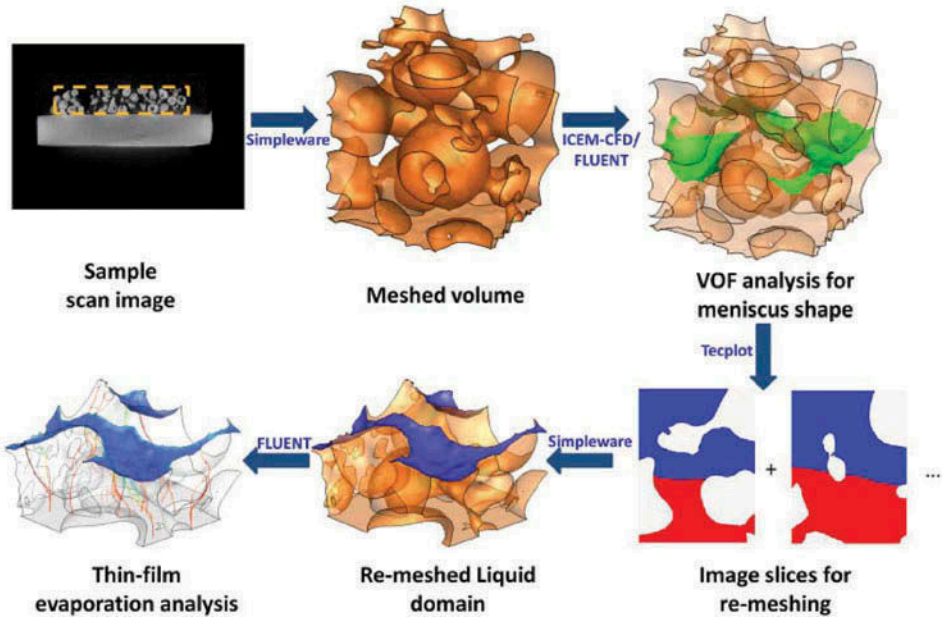

Figure 6 Direct simulation of evaporative heat transfer from a sintered wick structure [70]. The typical workflow for microtomography-based visualization, 3D reconstruction, meshing, meniscus shape prediction, and subsequent evaporation analysis is shown. Reprinted from *International Journal of Heat and Mass Transfer*, K.K. Bodla, J.Y. Murthy, and S.V. Garimella, Evaporation Analysis of Sintered Wick Microstructures Vol. 58, pp. 300−311, Copyright (2013), with permission from Elsevier.

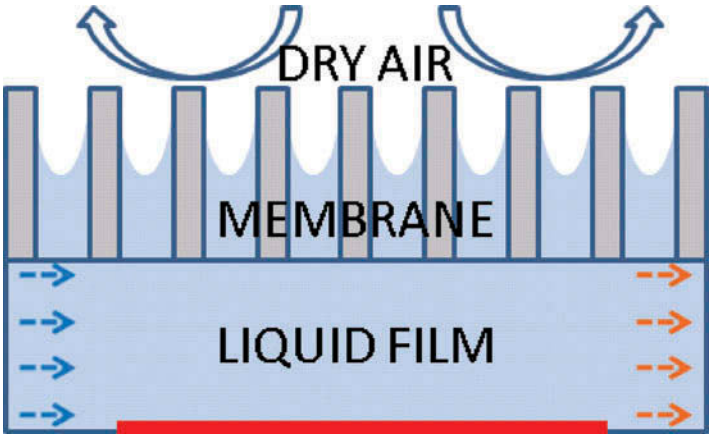

Figure 7 Membrane-based evaporation/perspiration system for enhancing evaporative heat and mass transfer using external gas assistance.

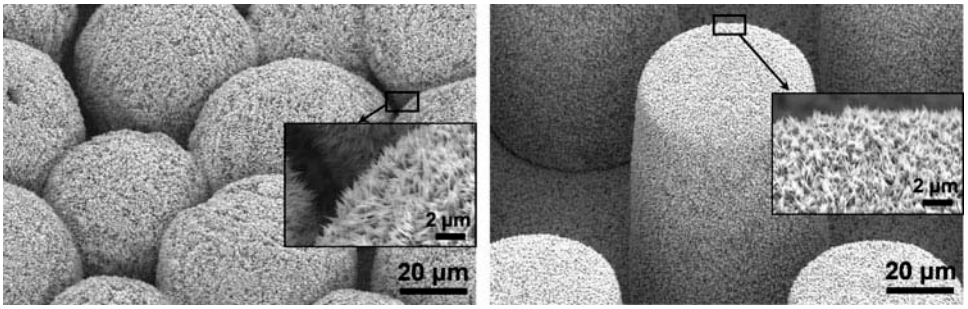

Figure 8 Micro/nanostructured evaporator surfaces for enhanced heat transfer.

reverse-engineering the design of microstructures via simulation of the physical fabrication processes, are reviewed in Bodla et al. [64]. Others researchers have machined wicking-type structures using lithographic techniques [15–17, 21, 27, 65]. Deposition and etching processes have been used to create nanostructured surfaces [22, 29]. In many approaches, the investigators have tried to mimic biological processes such as perspiration via membranes [77–81] as in Figure 7, dual-roughness structures [8, 22, 23, 26] as in Figure 8, and chemical modification [82] using temperature to control the morphology of polymers grafted to a surface. Confining the process to microchannels, with both smooth and micro/nanostructured walls, has also been a much-studied route [83, 84]. Perhaps the oldest strategy is to just spray the liquid in the form of very fine droplets onto the surface. Despite these efforts, there is still no unifying framework for microstructure design, manufacturing techniques, and ultimate characterization and comparison of performance enhancement.

SYNTHESIS AND OUTLINE FOR FUTURE RESEARCH

We are now in a position to organize past efforts and future research directions along a set of general principles. To maximize evaporation, we would like to maximize the region with least resistance to evaporation, and we need to be able to deliver liquid to that region

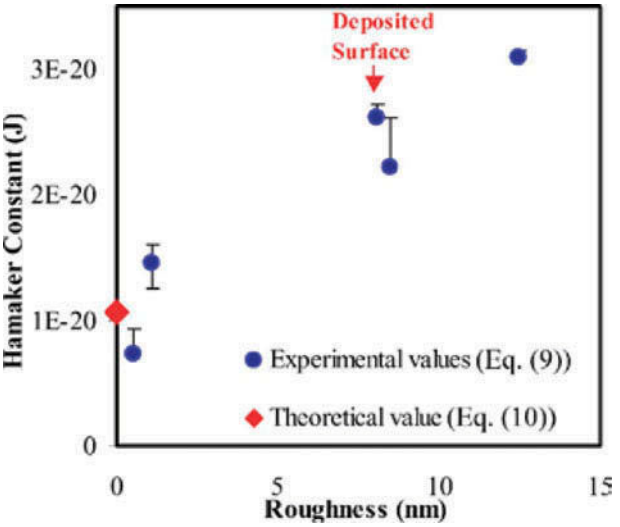

Figure 9 Effective Hamaker constant as a function of average surface roughness. The theoretical value is obtained for a smooth surface from Eq. (3) [22]. Reprinted with permission M. Ojha, A. Chatterjee, G. Dalakos, P.C. Wayner, Jr., and J.L. Plawsky, Role of Solid Surface Structure on Evaporative Phase Change from a Completely Wetting Corner Meniscus, *Physics of Fluids*, Vol. 22, 052101, 2010. Copyright 2010, AIP Publishing LLC.

in sufficient quantity to feed the evaporation. This requires control of the intermolecular force interaction and, as a consequence, the apparent contact angle and interfacial tension. Ideally, one would want a perfectly wetting fluid to insure a spreading, thin film over the entire surface. If, for simplicity, we choose only a van der Waals fluid, there are several more generalizations we can make. Dzyaloshinskii, Lifshitz, and Pitaevskii's theory indicates that we need to choose the dielectric properties of the substrate and liquid to adjust the Hamaker constant so it is large and negative, thereby insuring perfect wettability. Because theory treats the materials as continua using the bulk dielectric constant and refractive index, we should be able to use nanostructures to alter the effective Hamaker constant as long as those structures are small relative to the primary absorption wavelength, λ_e, controlling the dispersion force. Random structures of this type have been shown to alter the effective Hamaker constant [20] as shown in Figure 9. Highly structured surfaces exploiting this effect are believed to be active in biological systems, such as the septae in gecko feet [85]. If systems composed of purely dielectric materials are insufficient, we can incorporate surface plasmon resonance effects by fabricating metallic nanostructures so that the fluid responds to electromagnetic fields.

Though we can choose fluids, materials, and force fields to alter the wetting, we still need to be able to deliver the liquid to the active evaporation zone and that is primarily accomplished via capillarity. We need a very large curvature gradient, in general, to provide the required pumping power. In most systems, there is a reservoir located a large distance (L) from the evaporation zone (relative to the film thickness near the contact line), so the capillary driving force will scale as $\sigma_{lv}\cos\theta_{eq}/d$. Here, θ_{eq} is the equilibrium contact angle the liquid makes with the solid surface. To increase the driving force, we can use wicks or surfaces that are structured on the microscale, creating local reservoirs between each structure that are separated by a much smaller distance, d. Unfortunately, increasing the driving force using microscale features also increases the hydrodynamic resistance that

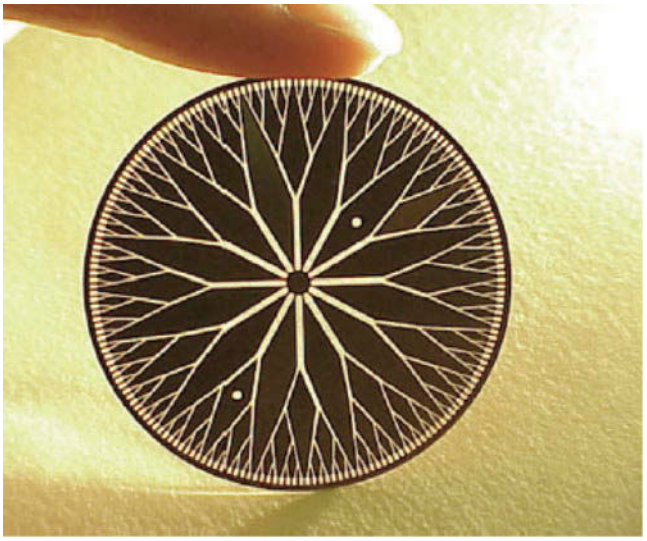

Figure 10 Fractal channel network for enhanced heat transfer [89, 90]. Reprinted from *Experimental Thermal and Fluid Science*, D. Pence, The Simplicity of Fractal-Like Flow Networks for Effective Heat and Mass Transport, Vol. 34, pp. 474-486, Copyright (2010); and *International Journal of Heat and Mass Transfer*, S. Salakij, J.A. Liburdy, D.V. Pence, and M. Apreotesi, Modeling in-situ Vapor Extraction during Convective Boiling in Fractal-Like Branching Microchannel Networks, Vol. 60, pp. 700−712, Copyright (2013), with permission from Elsevier.

scales as $\mu_{\text{liq}} L u_{\text{liq}}/d^2$ where μ_{liq} is the liquid viscosity and u_{liq} is a measure of the liquid velocity that can be related to the mass flux needed to give a desired evaporation rate. By equating the driving force and resistance, the velocity with which we can deliver fluid scales as $u_{\text{liq}} = \sigma_{lv}\cos\theta_{\text{eq}} d/\mu_{\text{liq}} L$ and so as d gets smaller, we choke off the flow. Thus, the microstructure pattern must be optimized and can become very complicated. An example is shown in Figure 10 where large, hierarchically etched microchannels would be used to feed micro- or nanostructured arrays that would fill the space between the channels.

Liquid properties change with temperature and, in particular, the interfacial tension decreases with temperature, so to achieve very high evaporation rates one must also overcome the Maragoni forces that tend to limit flow toward the evaporation region. One way to combat this effect is to provide a gradient in the intermolecular force field using surface structures or chemical modification that opposes the change in interfacial tension. However, such a static surface is optimized for only one condition. An alternative technique is to use liquid mixtures and allow differential evaporation to establish a concentration-driven Marangoni force that opposes the temperature-driven force [31–35]. This provides for a self-regulating system, but large concentration gradients would generally be required, opening the doorway to additional complications such as multiple liquid phases and azeotropes in nonideal mixtures.

A comprehensive strategy to maximize evaporation would thus employ tuned bulk material dielectric properties coupled with nanostructures to control the wetting behavior of the liquid on the submicrometer scale, microscale patterning to enhance the capillary driving force within the bulk meniscus, and surface modifications or liquid mixtures to combat temperature gradient-induced fluid flow away from the active evaporation zone.

It should be noted that as the nanostructures controlling liquid film morphology and transport become optimized for the best performance in liquid phase (i.e., thinning the film

and effectively pumping it to the evaporating zone without dry-outs), the evaporation may ultimately become limited by the ability to remove vapor molecules from the evaporating interface to the ultimate mass sink. The vapor-phase resistance has received little attention to date, but some fundamental studies and innovative structures—for example, in the gas-assisted thin-film evaporation [71, 79, 86, 87]—have been undertaken and developed. This issue is likely to receive increasing attention in the coming years as we realize that all rate-limiting resistances will have to be carefully minimized to achieve the next level in performance.

Lastly, a dominant majority of studies on thin evaporation is limited to the steady-state behavior, which is simpler to control and investigate both theoretically and experimentally. However, transient operation of evaporating films may provide an untapped resource for exploring new operating modes with even higher instantaneous and time-averaged heat dissipation capabilities and should not be ignored in the future.

FUTURE RESEARCH NEEDS

Though investigators have worked both experimentally and theoretically probing individual components of the strategies listed above, little attention has been given about how to integrate all the elements into an optimized system. This is especially true given what we now know and can fabricate on the atomistic, nanometer, and micrometer scales. Discussions during the workshop indicated that to proceed along these lines and further our research efforts, the community requires the following:

1. Consensus on a standard set of fluids that span the range from simple van der Waals fluids such as pentane or refrigerant, to polar fluids such as ethanol or isopropanol, and finally to very complicated fluids like water and mixtures that can be investigated both individually and in combination. This would help the experimentalists provide a standard set of data but also the continuum and molecular modelers who could progress steadily from the simplest to the most complicated scenarios knowing that there is reliable data to compare with.
2. Consensus on standard set of materials that span the range of dielectric properties of potential interest including pure dielectric materials, semiconducting materials, and metals. These materials should be simple enough that we can routinely process them at both the nanoscale and microscale using available semiconducting processing methods or via solution-based methods. If we are required to develop different processing recipes from scratch every time, work will be delayed.
3. Well defined, fundamental studies of how the fluid, material, and structure combine to control wetting, spreading, pumping, and evaporation. This may require the community to develop an overall experimental matrix that a number of members can begin to fill in.
4. A consensus definition of contact angle, a scale-dependent property that depends upon many variables including the superheat.
5. A consensus definition on how we characterize multiscale surface structure, what we mean by *roughness*, and what is it about the roughness or structure that enhances the transport. Though we have a good idea of the process on the microscale where we can treat the liquid as a continuum, we do not have such an understanding at the nanoscale. Here, experimentalists and molecular simulators must come together. For example, is it the average roughness, the peak-to-valley roughness, or the lateral correlation length

between features or the interaction between scales of roughness that is most important, and how do we quantify it?

6. A set of well-defined patterns fabricated from the suite of specified materials that multiple investigators can study. The idea would be to develop a database for how these systems behave by combining observations and simulations from a number of groups around the world.
7. Much more interaction between experimentalists, theorists, and simulators. The evaporation process is inherently multiscale, and models developed at the continuum scale suffer from an inadequate specification of the boundary conditions at the molecular scale. This includes curvature, thickness, and contact angle at the contact line as well as hydrodynamic slip at the solid liquid interface, especially when nanostructures are present. Phenomena such as nucleation may even require information at the atomic scale so that we can understand why one crystal structure or face performs so much better than another.

CONCLUSIONS

Evaporation from thin films is a key feature of many processes, including energy conversion, microelectronics cooling, boiling, perspiration, and self-assembly operations. We are now at a point where we believe that the underlying physics of the phenomena are well understood and that the interfacial temperature, interfacial composition, disjoining pressure, surface tension, interface curvature, interface instabilties, and bulk movement of the vapor phase all interact to govern the rate of evaporation. The process is an inherently dynamic one and so past quasisteady approaches may no longer capture all of the essential physics of the problem. Transient analyses will be required, as will the ability to engineer surfaces and fluids to control these transient interfaces.

Evidence suggests that altering the surface chemistry and surface topography on the micro- and nanoscales can be used to dramatically enhance vaporization. Though minimizing device dimensions through microfabrication and tailoring the substrate properties and liquid–solid interactions via surface nanoengineering have seen significant advancements and are becoming within the limits of our capabilities, a capability for effective removal of the vapor phase from the evaporating interface to the far ambient remains a fundamental challenge that calls for innovative process organization and in-depth understanding of gas-phase fluid mechanics and mass transfer in confined geometries.

Experimental characterization techniques such as X-ray microtomography and laser-scanning confocal microscopy will provide 3D topological and microstructural details of porous media and engineered surfaces. Transient, multiwavelength interferometry will provide the same level of information regarding the in situ disjoining pressure and thin-film thickness profiles. Reconstruction of these materials and films with feature-preserving, adaptive meshing algorithms will allow for accurate, on-demand characterization of pertinent evaporation and heat transport properties, rather than relying on reduced-order or empirically based characterization approaches.

ACKNOWLEDGMENTS

The authors express their appreciation to Professors Yoav Peles and Evelyn Wang for organizing the workshop and to MIT for hosting the workshop. JLP would also like to thank NASA and the CVB program.

FUNDING

This article is the result of a workshop supported by US Department of Energy ARPA-E (Grant No. DE-AR0000363), the US National Science Foundation (Grant No. 1261824), and the Office of Naval Research (Grant No. N00014-13-1-0324).

REFERENCES

1. B.V. Deryagin, S.V. Nerpin, and N.V. Churaev, To the Theory of Liquid Evaporation from Capillaries, *Kolloidn. Zh.*, Vol. 26, pp. 301–307, 1964.
2. O.A. Kiseleva, V.M. Starov, and N.V. Churaev, Calculations of Film Flow under the Action of a Temperature Gradient in Conical Capillaries, *Kolloidn. Zh.*, Vol. 39, pp. 1164–1167, 1977.
3. R.W. Schrage, *A Theoretical Study of Interphase Mass Transfer*, Columbia University Press, New York, 1953.
4. L. Cao, H.H. Hu, and D. Gao, Design and Fabrication of Micro-Textures for Inducing a Superhydrophobic Behavior on Hydrophilic Materials, *Langmuir*, Vol. 23, pp. 4310–4314, 2007.
5. L. Cao, T.P. Price, M. Weiss, and D. Gao, Super Water- and Oil-Repellent Surfaces on Intrinsically Hydrophilic and Oleophilic Porous Silicon Films, *Langmuir*, Vol. 24, pp. 1640–1643, 2008.
6. X. M. Li, D. Reinhoudt, and M. Crego-Calama, What Do We Need for a Superhydrophobic Surface? A Review on the Recent Progress in the Preparation of Superhydrophobic Surfaces, *Chemical Society Reviews*, Vol. 36, pp. 1350–1368, 2007.
7. F. Zhang, W.B. Zhang, Z. Shi, D. Wang, J. Jin, and L. Jiang, Nanowire-Haired Inorganic Membranes with Superhydrophilicity and Underwater Ultralow Adhesive Superoleophobicity for High-Efficiency Oil/Water Separation, *Advanced Materials*, Vol. 25, pp. 4192–4198, 2013.
8. Y. Nam, S. Sharratt, C. Byon, S.J. Kim, and Y.S. Ju, Fabrication and Characterization of the Capillary Performance of Superhydrophilic Cu Micropost Arrays, *Journal of Microelectromechanical Systems*, Vol. 19, pp. 581–588, 2010.
9. J.L. Plawsky, J.K. Kim, and E.F. Schubert, Review: Engineered Nanoporous and Nanostructured Films, *Materials Today*, Vol. 12, pp. 36–45, 2009.
10. X. Deng, L. Mammen, H.-J. Butt, and D. Vollmera, Candle Soot as a Template for a Transparent Robust Superamphiphobic Coating, *Science*, Vol. 335, pp. 67–70, 2012.
11. A. Susarrey-Arce, Á.G. Marín, H. Nair, L. Lefferts, J.G.E. Gardeniers, D. Lohse, and A. van Houselt, Absence of an Evaporation-Driven Wetting Transition on Omniphobic Surfaces, *Soft Matter*, Vol. 8, pp. 9765–9770, 2012.
12. J.L. Plawsky, M. Ojha, A. Chatterjee, and P.C. Wayner, Jr., Review of the Effects of Surface Topography, Surface Chemistry, and Fluid Physics on Evaporation at the Contact Line, *Chemical Engineering Communications*, Vol. 196, pp. 658–696, 2008.
13. A.E. Bergles, Recent Developments in Enhanced Heat Transfer, *Heat and Mass Transfer*, Vol. 47, pp. 1001–1008, 2011.
14. R. Xiao and E.N. Wang, Microscale Liquid Dynamics and the Effect on Macroscale Propagation in Pillar Arrays, *Langmuir*, Vol. 27, pp. 10360–10364, 2011.
15. W. Liu, Y. Li, Y. Cai, and D.P. Sekulic, Capillary Rise of Liquids over a Microstructured Solid Surface, *Langmuir*, Vol. 27, pp. 14260–14266, 2011.
16. L. Courbin, E. Denieul, E. Dressaire, M. Roper, A. Ajdari, and H. A. Stone, Imbibition by Polygonal Spreading on Microdecorated Surfaces, *Nature Materials*, Vol. 6, pp. 661–664, 2007.
17. R. Ranjan, J.Y. Murthy, and S.V. Garimella, Analysis of the Wicking and Thin-Film Evaporation Characteristics of Microstructures, *Journal of Heat Transfer*, Vol. 131, 101001, 2009.
18. R. Manglik, On the Advancements in Boiling, Two-Phase Flow Heat Transfer, and Interfacial Phenomena, *Journal of Heat Transfer*, Vol. 128, pp. 1237–1242, 2006.
19. S.C. Maroo and J.N. Chung, A Possible Role of Nanostructured Ridges on Boiling Heat Transfer Enhancement, *Journal of Heat Transfer*, 041501, 2013.

20. Y. Nam, E. Aktinol, V.K. Dhir, and Y.S. Ju, Single Bubble Dynamics on a Superhydrophilic Surface With Artificial Nucleation Sites, *International Journal of Heat and Mass Transfer*, Vol. 54, pp. 1572–1577, 2011.
21. D. Quere, Wetting and Roughness, *Annual Review of Materials Research*, Vol. 38, pp. 71–99, 2008.
22. M. Ojha, A. Chatterjee, G. Dalakos, P.C. Wayner, Jr., and J.L. Plawsky, Role of Solid Surface Structure on Evaporative Phase Change from a Completely Wetting Corner Meniscus, *Physics of Fluids*, Vol. 22, 052101, 2010.
23. Y. Nam and Y.S. Ju, A Comparative Study of the Morphology and Wetting Characteristics of Micro/Nanostructured Cu Surfaces for Phase Change Heat Transfer Applications, *Journal of Adhesion Science and Technology*, Vol. 27, pp. 2163–2176, 2013.
24. R. Ranjan, S.V. Garimella, and J.Y. Murthy, Assessment of Nanostructured Capillary Wicks for Passive Two-Phase Heat Transport, *Nanoscale and Microscale Thermophysical Engineering*, Vol. 15, pp. 179–194, 2011.
25. S.J. Gokhale, J.L. Plawsky, and P.C. Wayner, Jr., Spreading, Evaporation, and Contact Line Dynamics of Surfactant-Laden Microdrops, *Langmuir*, Vol. 21, pp. 8188–8197, 2005.
26. M. Ojha, A. Chatterjee, F. Mont, E.F. Schubert, P.C. Wayner, Jr., and J.L. Plawsky, The Role of Solid Surface Structure on Dropwise Phase Change Processes, *International Journal of Heat and Mass Transfer*, Vol. 53, pp. 910–922, 2010.
27. F. Barberis and M. Capurro, Wetting in the Nanoscale: A Continuum Mechanics Approach, *Journal of Colloid and Interface Science*, Vol. 326, pp. 201–210, 2008.
28. K. Kamrin, M.Z. Bazant, and H.A. Stone, Effective Slip Boundary Conditions for Arbitrary Periodic Surfaces: The Surface Mobility Tensor, *Journal of Fluid Mechanics*, Vol. 658, pp. 409–437, 2010.
29. J.P. Rothstein, Slip on Superhydrophobic Surfaces, *Annual Review of Fluid Mechanics*, Vol. 42, pp. 89–109, 2010.
30. N. Miljkovic, R. Enright, and E.N. Wang, Effect of Droplet Morphology on Growth Dynamics and Heat Transfer during Condensation on Superhydrophobic Nanostructured Surfaces, *ACS Nano*, Vol. 6, pp. 1776–1785, 2012.
31. D.M. Pratt and K.D. Kihm, Binary Fluid Mixture and Thermocapillary Effects on the Wetting Characteristics of a Heated Curved Meniscus, *Journal of Heat Transfer*, Vol. 125, pp. 867–874, 2003.
32. R. Savinoa, N. di Francescantonio, R. Fortezza, and Y. Abe, Heat Pipes with Binary Mixtures and Inverse Marangoni Effects for Microgravity Applications, *Acta Astronomica*, Vol. 61, pp. 16–26, 2007.
33. N. di Francescantonio, R. Savino, and Y. Abe, New Alcohol Solutions for Heat Pipes: Marangoni Effect and Heat Transfer Enhancement, *International Journal of Heat and Mass Transfer*, Vol. 51, pp.6199–6207, 2008.
34. K.M. Armijo and V.P. Carey, An Experimental Study of Heat Pipe Performance Using Binary Mixture Fluids That Exhibit Strong Concentration Marangoni Effects, *Journal of Thermal Science and Engineering Applications*, Vol. 3, 031003, 2011.
35. S.S. Panchamgam, J.L. Plawsky, and P.C. Wayner, Jr., Spreading Characteristics and Microscale Evaporative Heat Transfer in an Ultrathin Film Containing a Binary Mixture, *Journal of Heat Transfer*, Vol. 128, pp. 1266–1275, 2006.
36. S.J. Gokhale, S.S. DasGupta, J.L. Plawsky, P.C. Wayner, Jr., Reflectivity Based Evaluation of the Coalescence of Two Condensing Drops and Shape Evolution of the Coalesced Drop, *Physical Review E*, Vol. 70, No. 5, 051610, 2004.
37. K. Ibrahem, M.F. Abd Rabbo, T. Gambaryan-Roisman, and P. Stephan, Experimental Investigation of Evaporative Heat Transfer Characteristics at the 3-Phase Contact Line, *Experimental Thermal and Fluid Science*, Vol. 34, pp. 1036–1041, 2010.
38. R. Raj, C. Kunkelmann, P. Stephan, J. Plawsky, and J. Kim, Contact Line Behavior for a Highly Wetting Fluid under Superheated Conditions, *International Journal of Heat and Mass Transfer*, Vol. 55, pp. 2664–2675, 2012.

39. K. Sefiane and C.A. Ward, Recent Advances on Thermocapillary Flows and Interfacial Conditions during the Evaporation of Liquids, *Advances in Colloid and Interface Science*, Vol. 134–135, pp. 201–223, 2007.
40. F. Su, H.B. Ma, X. Han, H. Chen, and B. Tian, Ultra-High Cooling Rate Utilizing Thin Film Evaporation, *Applied Physics Letters*, Vol. 101, 113702, 2012.
41. C.P. Migliaccio, H.K. Dhavaleswarapu, and S.V. Garimella, Temperature Measurements Near the Contact Line of an Evaporating Meniscus V-Groove, *International Journal of Heat and Mass Transfer*, Vol. 54, pp. 1520–1526, 2011.
42. H.B. Ma, P. Cheng, and B. Borgmeyer, Fluid Flow and Heat Transfer in the Evaporating Thin Film Region, *Microfluidics and Nanofluidics*, Vol. 4, pp. 237–243, 2008.
43. H.K. Dhavalewsarapu, S.V. Garimella, and J.Y. Murthy, Microscale Temperature Measurements near the Triple Line of an Evaporating Thin Liquid Film, *Journal of Heat Transfer*, Vol. 131, 061501, 2009.
44. G. Ramon and A. Oron, Capillary Rise of a Meniscus with Phase Change, *Journal of Colloid and Interface Science*, Vol. 327, pp. 145–151, 2008.
45. V.S. Nikolayev, Dynamics of the Triple Contact Line on a Nonisothermal Heater at Partial Wetting, *Physics of Fluids*, Vol. 22, 082105, 2010.
46. C. Yan and H.B. Ma, Analytical Solutions of Heat Transfer and Film Thickness in Thin Film Evaporation, *Journal of Heat Transfer*, Vol. 135, 031501, 2013.
47. W. Ren, D. Hu, and E. Weinan, Continuum Models for the Contact Line Problem, *Physics of Fluids*, Vol. 22, 102103, 2010.
48. H. Wang, S.V. Garimella, and J.Y. Murthy, Characteristics of an Evaporating Thin Film in a Microchannel, *International Journal of Heat and Mass Transfer*, Vol. 50, pp. 3933–3942, 2007.
49. H.K. Dhavaleswarapu, J.Y. Murthy, and S.V. Garimella, Numerical Investigation of an Evaporating Meniscus in a Channel, *International Journal of Heat and Mass Transfer*, Vol. 55, pp. 915–924, 2012.
50. V.S. Ajaev, T. Gambaryan-Roisman, and P. Stephan, Static and Dynamic Contact Angles of Evaporating Liquids on Heated Surfaces, *Journal of Colloid and Interface Science*, Vol. 342, pp. 550–558, 2010.
51. V.P. Carey and A.P. Wemhoff, Disjoining Pressure Effects in Ultra-Thin Liquid Films in Micropassages—Comparison of Thermodynamic Theory With Predictions of Molecular Dynamics Simulations, *Journal of Heat Transfer*, Vol. 128, pp. 1276–1284, 2006.
52. S.C. Maroo and J.N. Chung, Heat Transfer Characteristics and Pressure Variation in a Nanoscale Evaporating Meniscus, *International Journal of Heat and Mass Transfer*, Vol. 53, pp. 3335–3345, 2010.
53. G. Nagayama, M. Kawagoe, A. Tokunaga, and T. Tsuruta, On the Evaporation Rate of Ultra-Thin Liquid Film at the Nanostructured Surface: A Molecular Dynamics Study, *International Journal of Thermal Sciences*, Vol. 49, pp. 59–66, 2010.
54. J. Liu, S. Chen, X. Nie, and M.O. Robbins, A Continuum–Atomistic Simulation of Heat Transfer in Micro- and Nano-Flows, *Journal of Computational Physics*, Vol. 227, pp. 279–291, 2007.
55. J.B. Freund, The Atomic Detail of an Evaporating Meniscus, *Physics of Fluids*, Vol. 17, 022104, 2005.
56. S. Narayanan, A.G. Fedorov, and Y. Joshi, Interfacial Transport of Evaporating Water Confined in Nanopores, *Langmuir*, Vol. 27, pp. 10666–10676, 2011.
57. V.P. Carey, *Liquid Vapor Phase Change Phenomena: An Introduction to the Thermophysics of Vaporization and Condensation Processes in Heat Transfer Equipment*, 2nd ed., Taylor & Francis, New York, 2007.
58. A.M. Benselam, S. Harmand, and K. Sefiane, Thermocapillary Effects on Steadily Evaporating Contact Line: A Perturbative Local Analysis, *Physics of Fluids*, Vol. 24, 072105, 2012.
59. A. Oron, S.H. Davis, and S.G. Bankoff, Long-Scale Evolution of Thin Liquid Films, *Reviews of Modern Physics*, Vol. 69, pp. 931–980, 1997.
60. V. Ajaev, Instability and Rupture of Thin Liquid Films on Solid Substrates, *Journal of Interfacial Phenomena and Heat Transfer*, Vol. 1, pp. 81–92, 2013.

61. S. Narayanan, A. Fedorov, and Y. Joshi, Interfacial Transport of Evaporating Water Confined in Nanopores, *Langmuir*, Vol. 27, pp. 10666–10676, 2011.
62. K.K. Bodla, J.Y. Murthy, and S.V. Garimella, Direct Simulation of Thermal Transport Through Sintered Wick Microstructures, *Journal of Heat Transfer*, Vol. 134, 012602, 2012.
63. K.K. Bodla, J.Y. Murthy, and S.V. Garimella, Evaporation Analysis in Sintered Wick Microstructures, *International Journal of Heat and Mass Transfer*, Vol. 61, pp. 729–741, 2013.
64. K.K. Bodla, J.A. Weibel, and S.V. Garimella, Advances in Fluid and Thermal Transport Property Analysis and Design of Sintered Porous Wick Microstructures, *Journal of Heat Transfer*, Vol. 135, 061202, 2013.
65. R. Ranjan, J.Y. Murthy, and S.V. Garimella, Marangoni Convection and Thin-Film Evaporation in Microstructured Wicks for Heat Pipes, *Journal of Heat Transfer*, Vol. 132, 080902, 2010.
66. R. Ranjan, J.Y. Murthy, S.V. Garimella, and U. Vadakkan, A Numerical Model for Transport in Flat Heat Pipes Considering Wick Microstructure Effects, *International Journal of Heat and Mass Transfer,* Vol. 54, pp. 153−168, 2011.
67. M.A. Hanlon and H.B. Ma, Evaporation Heat Transfer in Sintered Porous Media, *Journal of Heat Transfer*, Vol. 125, pp. 644–653, 2003.
68. R. Ranjan, J.Y. Murthy, and S.V. Garimella, A Microscale Model for Thin-Film Evaporation in Capillary Wick Structures, *International Journal of Heat and Mass Transfer*, Vol. 54, pp. 169–179, 2011.
69. Y. Nam, S. Sharratt, G. Cha, and Y.S. Ju, Characterization and Modeling of the Heat Transfer Performance of Nanostructured Cu Micropost Wicks, *Journal of Heat Transfer*, Vol. 133, 101502, 2011.
70. K.K. Bodla, J.Y. Murthy, and S.V. Garimella, Evaporation Analysis of Sintered Wick Microstructures, *International Journal of Heat and Mass Transfer*, Vol. 61, pp. 729–741, 2013.
71. S. Narayanan, A. Fedorov, and Y. Joshi, Gas-Assisted Thin-Film Evaporation from Confined Spaces for Dissipation of High Heat Fluxes, *Nanoscale and Microscale Thermophysical Engineering*, Vol. 13, pp. 30–53, 2009.
72. P.C. Wayner, Jr., Interfacial Profile in the Contact Line Region of a Finite Contact Angle System, *Journal of Colloid and Interface Science*, Vol. 77, pp. 495–500, 1980.
73. F. Mugele and J.-C. Baret, Electrowetting: From Basics to Applications, *Journal of Physics: Condensed Matter*, Vol. 17, pp. R705–R774, 2005.
74. S. Basu and M.M. Sharma, Measurements of Critical Disjoining Pressure for Dewetting of Solid Surfaces, *Journal of Colloid and Interface Science*, Vol. 181, pp. 443–455, 1996.
75. J.N. Israelachvili, *Intermolecular and Surface Forces*, 3rd ed., Academic Press, San Diego, CA, 2011.
76. R. Marek and J. Straub, Analysis of the Evaporation Coefficient and the Condensation Coefficient of Water, *International Journal of Heat and Mass Transfer*, Vol. 44, pp. 39–53, 2001.
77. X. Dai, F. Yang, R. Yang, Y.-C. Lee, and C. Li, Micromembrane-Enhanced Capillary Evaporation, *International Journal of Heat and Mass Transfer*, Vol. 64, pp. 1101–1108, 2013.
78. S. Narayanan, A.G. Fedorov, and Y.K. Joshi, On-Chip Thermal Management of Hotspots Using a Perspiration Nanopatch, *Journal of Micromechanics and Microengineering*, Vol. 20, 075010, 2010.
79. X. Dai, F. Yang, Y.-C. Lee, R. Yang, and C. Li, Micromembrane Enhanced Capillary Evaporation, *International Journal of Heat and Mass Transfer*, Vol. 64, pp. 1101–1108, 2013.
80. S. Narayanan, A. Fedorov, and Y. Joshi, Heat And Mass Transfer during Evaporation of Thin Liquid Films Confined by Porous Membrane Subjected to Air Jet Impingement, *International Journal of Heat and Mass Transfer*, Vol. 58, pp. 300–311, 2013.
81. T. Sun, G. Wang, L. Feng, B. Liu, Y. Ma, L. Jiang, and D. Zhu, Reversible Switching between Superhydrophilicity and Superhydrophobicity, *Angewandte Chemie International Edition*, Vol. 43, pp. 357–360, 2004.

82. F. Yang, X. Dai, Y. Peles, P. Cheng, and C. Li, Can Multiple Flow Boiling Regimes Be Reduced into a Single One in Microchannels?, *Applied Physics Letters*, Vol. 103, 043122, 2013.
83. J.-J. Zhao, M. Huang, Q. Mina, D.M. Christopher, and Y.-Y. Duan, Thermal Resistance for Thin-Film Evaporation in Microchannels, *Nanoscale and Microscale Thermophysical Engineering*, Vol. 15, pp. 105–122, 2011.
84. G.S. Hwang, Y. Nam, E. Fleming, P. Dussinger, Y.S. Ju, and M. Kaviany, Multi-Artery Heat Pipe Spreader: Experiment, *International Journal of Heat and Mass Transfer*, Vol. 53, pp. 2662–2669, 2010.
85. K. Autumn, M. Sitti, Y.A. Liang, A.M. Peattie, W.R. Hansen, S. Sponberg, T.W. Kenny, R. Fearing, J.N. Israelachvili, and R.J. Full, Evidence for Van Der Waals Adhesion in Gecko Setae, *Proceedings of the National Academy of Sciences*, Vol. 99, pp. 12252–12256, 2002.
86. A. Bar-Cohen, G. Sherwood, M. Hodes, and G. Solbreken, Gas-Assisted Evaporative Cooling of High Density Electronic Modules, *IEEE Transactions on Components, Packaging, and Manufacturing Technology, Part A*, Vol. 18, pp. 502–509, 1995.
87. E.Y. Gatapova and O.A. Kabov, Shear-Driven Flows of Locally Heated Liquid Films, *International Journal of Heat and Mass Transfer*, Vol. 51, 4797–4810, 2008.
88. Y.-T. Cheng, D.E. Rodak, A. Angelopoulos, and T. Gacek, Microscopic Observations of Condensation of Water on Lotus Leaves, *Applied Physics Letters*, Vol. 87, pp. 194112–194113, 2005.
89. D. Pence, The Simplicity of Fractal-Like Flow Networks for Effective Heat and Mass Transport, *Experimental Thermal and Fluid Science*, Vol. 34, pp. 474–486, 2010.
90. S. Salakij, J.A. Liburdy, D.V. Pence, and M. Apreotesi, Modeling in-situ Vapor Extraction during Convective Boiling in Fractal-Like Branching Microchannel Networks, *International Journal of Heat and Mass Transfer*, Vol. 60, pp. 700–712, 2013.